JACS
JOURNAL OF THE AMERICAN CHEMICAL SOCIETY

Communication

pubs.acs.org/JACS

Potentiometric Measurements of Semiconductor Nanocrystal Redox Potentials

Gerard M. Carroll, Carl K. Brozek, Kimberly H. Hartstein, Emily Y. Tsui, and Daniel R. Gamelin*

Department of Chemistry, University of Washington, Seattle, Washington 98195-1700, United States

Supporting Information

ABSTRACT: A potentiometric method for measuring redox potentials of colloidal semiconductor nanocrystals (NCs) is described. Fermi levels of colloidal ZnO NCs are measured *in situ* during photodoping, allowing correlation of NC redox potentials and reduction levels. Excellent agreement is found between electrochemical and optical redox-indicator methods. Potentiometry is also reported for colloidal CdSe NCs, which show more negative conduction-band-edge potentials than in ZnO. This difference is highlighted by spontaneous electron transfer from reduced CdSe NCs to ZnO NCs in solution, with potentiometry providing a measure of the inter-NC electron-transfer driving force. Future applications of NC potentiometry are briefly discussed.

The redox potentials of colloidal semiconductor nanocrystals (NCs) play central roles in many current and envisioned technologies. For example, electron-transfer (ET) kinetics and reaction spontaneity for NC-sensitized solar photocatalysis are governed by the redox potentials of the NC photoabsorbers.[1−6] Likewise, relative potentials of band-like and surface-trapped electronic configurations dictate NC electronic doping,[7] which governs the utility of NCs for electronic and optoelectronic technologies such as photovoltaics.[8,9] Although critical for many target applications, *in situ* measurements of colloidal NC redox potentials have proven challenging.

Cyclic voltammetry (CV) is the most commonly employed electrochemical technique for measuring colloidal NC redox potentials.[10−12] Irreversibility of NC CV waves, low current-to-NC ratios, redox-active surface states, and surface-composition inhomogeneities have all been found to complicate solution-phase NC electrochemistry. CV measurements of NCs immobilized on electrode surfaces have been successful,[12−15] but NC redox potentials are very sensitive to their surface chemistry,[16,17] and the redox potentials of the same NCs as free-standing colloids may therefore differ substantially. As a consequence of these complications, it is common for driving forces of ET reactions involving colloidal semiconductor NCs to be discussed in terms of band-edge potentials estimated from vacuum ionization and electron-affinity measurements, often of the corresponding bulk material. Although this approach has powerful intuitive value, observations[16,18] that altering surface ligation alone can shift NC band edges by as much as 1 eV highlight the need for *in situ* redox measurements of colloidal NCs in their native form. Here, we report a potentiometric method for measuring colloidal NC redox potentials. Potentiometry has been a valuable tool in metal nanoparticle research.[19] By coupling potentiometry with optical detection of conduction-band (CB) electrons in colloidal semiconductor NCs generated via photodoping,[20,21] redox potentials associated with these electrons can be deduced. As a simple proof of concept, we show that our colloidal CdSe NCs have CB-edge potentials more negative than our ZnO NCs, leading to spontaneous inter-NC ET from photoreduced CdSe NCs to ZnO NCs in solution. Additional mechanistic details are revealed by the transient open-circuit potentials.

Figure 1 illustrates the apparatus used to measure Fermi levels (E_F) during NC photodoping. In an airtight optical cuvette, solutions of NCs under N_2 atmosphere are photoreduced using hole quenchers.[7] The average number of CB electrons per NC ($\langle n \rangle$) is quantified during photodoping using absorption spectroscopy. Simultaneously, electrodes in the NC solution track changes in E_F under galvanostatic (I = 0 A) control, i.e., the potentiostat biases the working electrode in response to the photoinduced increase in E_F (Figure 1, right). The electrode and solution E_F remain equivalent at all times. Consequently, no depletion region at the electrode/electrolyte interface develops, and the recorded half-cell potential represents E_F of the NC suspension.[19] From these combined data, NC redox potentials at various electron densities can be determined. Accurate transient potentiometry requires a stable reference electrode. We use a leakless Ag/AgCl reference electrode, which avoids instabilities due to solution contamination, ionic activity, or electrode/electrolyte junction potentials (see Supporting Information (SI)). To account for

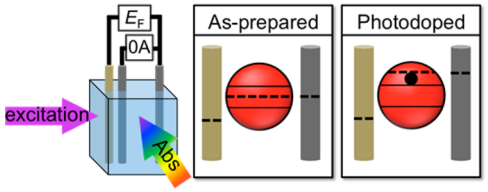

Figure 1. Apparatus used to collect potentiometric and absorption data during colloidal NC photodoping (left). Set to 0 A, the galvanostatic cell measures the solution potential during NC photodoping. NC absorption is measured simultaneously. The working electrode (gray) responds to changes in Fermi level upon NC photodoping.

Received: January 26, 2016
Published: March 15, 2016

DOI: 10.1021/jacs.6b00936
J. Am. Chem. Soc. 2016, 138, 4310−4313

possible electrochemical drift, CVs of an internal standard (cobaltocenium hexafluorophosphate, $[Cp_2Co][PF_6]$) were collected before and after most experiments. Drift was generally very small (<∼10 mV). All data are referenced experimentally to the ferrocenium/ferrocene couple (Fc^+/Fc, see SI).

Figure 2A plots E_F and the absorbance at λ = 1000 nm (A_{1000}) measured simultaneously during ZnO NC photodoping

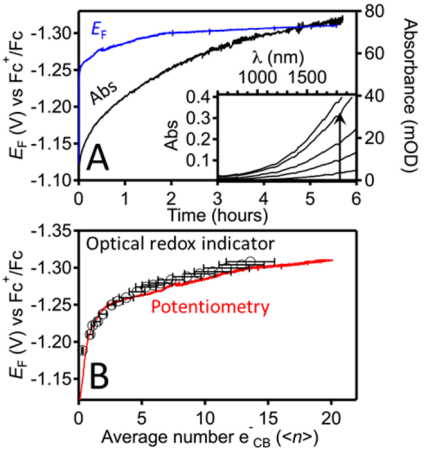

Figure 2. (A) Potentiometry (blue) and electronic absorption (black, λ = 1000 nm) data collected during photodoping of d = 6.8 nm ZnO NCs (2 μM) using EtOH as the hole quencher. A 14:1 THF/toluene solution of 0.1 M tetrabutylammonium hexafluorophosphate ($[Bu_4N][PF_6]$), 660 μM $[Cp_2Co][PF_6]$ was irradiated at 340 nm (12 mW) while stirring. The inset shows NIR absorption spectra of the same ZnO NCs growing with increasing $\langle n \rangle$. (B) Plot of E_F vs $\langle n \rangle$ for photodoped ZnO NCs derived from potentiometric (curve) and ORI (circles) methods. $\langle n \rangle$ was determined spectroscopically (see SI). The error bars represent $\pm \sigma$ from the mean. E_F is referenced to the Fc^+/Fc redox couple.

using ethanol as the hole quencher.[22,23] A_{1000} increases with ZnO photoexcitation, reflecting photodoping.[21,24−26] Concomitantly, E_F becomes more negative. From the per-electron extinction at λ = 1000 nm ($\varepsilon_{1000} = 1097\langle n \rangle^{0.7}$ M^{-1} cm^{-1}, see SI), $\langle n \rangle \approx 20$ e^-_{CB}/NC at its maximum ($\langle n_{max} \rangle$), corresponding to an average electron density of $\langle N_{max} \rangle \approx 1.21 \times 10^{20}$ cm^{-3}, in agreement with previous reports.[7,21,23,26] Because E_F and A_{1000} were measured simultaneously, it is valuable to plot E_F against $\langle n \rangle$ as shown in Figure 2B. E_F rises steeply at ∼ −70 mV/$\langle n \rangle$ between $\langle n \rangle$ = 0 and 2, after which its rise decreases to ∼ −4 mV/$\langle n \rangle$ until photodoping is complete.

It is instructive to compare these potentiometric data with those obtained using a solvated optical redox indicator (ORI),[1−3] an approach we applied recently to monitor ZnO NC photodoping.[27] Here, E_F is measured during photodoping using the optically detected equilibrium constant of a solvated redox couple that is also in equilibrium with the NCs. For the present comparison, ORI data were collected while photodoping the same ZnO NCs as probed electrochemically, under the same experimental conditions, and the ratio $[Cp_2Co^+]/[Cp_2Co]$ measured spectrophotometrically to determine E_F. These results are included in Figure 2B. The two methods yield nearly indistinguishable results.

Despite yielding the same results, potentiometry offers an important advantage over the ORI method: Potentiometry circumvents the need for a transparent spectroscopic window in which to monitor the ORI (e.g., for Cp_2Co, $\lambda_{probe} \approx$ 500 nm). Because of this advantage, the redox potentials of narrower-gap NCs can be readily monitored potentiometrically, making this the more general approach. As proof of concept, potentiometry and absorption were measured simultaneously during photodoping of CdSe NCs (with absorption overlapping that of Cp_2Co). Figure 3A plots electronic absorption spectra of

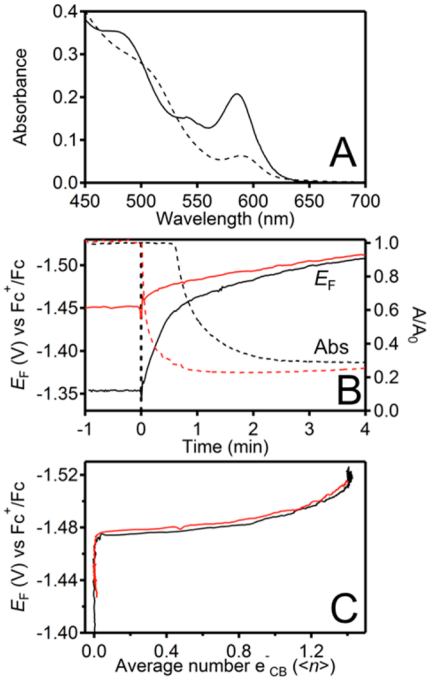

Figure 3. (A) Electronic absorption spectra of as-prepared (solid) and photodoped (dashed) d = 4.1 nm CdSe NCs. Experiments were performed using a 2:1 THF:toluene solution of NCs (0.9 μM), 0.05 M $[Bu_4N][PF_6]$, and 0.15 M trioctylphosphine oxide (TOPO). Photodoping used continuous 50 mW/cm^2 405 nm irradiation and $Na[Et_3BH]$ (200 μM) as the hole quencher. CB electrons are compensated by Na^+ and H^+.[21] (B) Transient potentiometric (E_F, solid) and excitonic absorption (A/A_0, dashed, λ = 590 nm) data collected simultaneously, using 0 (red) and 60 μM (black) $[Cp_2Co][PF_6]$, before (t < 0) and during ($t \geq 0$) 405 nm irradiation with constant stirring. E_F is referenced to the Fc^+/Fc couple. (C) Plot of E_F vs $\langle n \rangle$ from the data of panel B. $\langle n \rangle$ was calculated from $\langle n \rangle = 2(1 - A/A_0)$.

undoped and maximally photodoped d = 4.1 nm CdSe NCs, photoexcited at 405 nm in the presence of $Na[Et_3BH]$ (hole quencher),[20,28] $[Bu_4N][PF_6]$ (electrolyte), and TOPO (NC stabilizer). Photodoping causes the first NC excitonic transition to bleach to $A/A_0 \approx 0.3$ (A_0 = absorbance before photodoping) and redshift slightly, consistent with prior results.[20] From the established linear relationship between $\langle n \rangle$ and A/A_0,[20,29] these data imply $\langle n_{max} \rangle$ = 1.4, again consistent with previous results.[20,30] Note that the CdSe NC photodoping experiment is considerably quicker than the ZnO NC photodoping experiment (Figure 2) because of ∼5 times greater photoexcitation rates, greater conversion yields using $[Et_3BH]^-$ hole quenchers,[21] and smaller $\langle n_{max} \rangle$ in the CdSe NCs.

Figure 3B plots E_F and A/A_0 data collected transiently during CdSe NC photodoping for two experiments: one performed with Cp_2Co^+ as an electron shuttle and internal redox standard and the other without Cp_2Co^+. Prior to irradiation, E_F and A/A_0 are both constant, but E_F is ∼100 mV more positive in the sample containing Cp_2Co^+. This difference reflects a small amount of Cp_2Co^+ reduction prior to deliberate CdSe

DOI: 10.1021/jacs.6b00936
J. Am. Chem. Soc. 2016, 138, 4310−4313

irradiation.[31] Upon irradiation of the sample without Cp_2Co^+, E_F immediately shifts more negative, reaching a value near −1.52 V vs Fc^+/Fc after 4 min. Similarly, A/A_0 decreases immediately, reaching a new value of ∼0.3. Upon irradiation of the sample with Cp_2Co^+, E_F again immediately shifts more negative, reaching a similar value near −1.52 V vs Fc^+/Fc after 4 min. Interestingly, the onset of CdSe photodoping (as indicated by the inflection in A/A_0) is clearly delayed by ∼40 s in the presence of Cp_2Co^+, even though E_F starts shifting more negative immediately upon photoexcitation. This delayed photodoping reflects E_F equilibration between the CdSe NCs and Cp_2Co^+/Cp_2Co redox couples, which initially strongly favors Cp_2Co^+ reduction. Reduction of Cp_2Co^+ by photodoped CdSe NCs continues until the CdSe CB-edge potential is reached, at which point both Cp_2Co^+ reduction and CdSe NC electron accumulation proceed simultaneously with further photoexcitation. This observation is an example of the new insights that can be gained from potentiometry in the time domain.

Figure 3C plots E_F vs $\langle n \rangle$ for both experiments of Figure 3B. Although E_F is very different for the two samples prior to photodoping, the onset of CdSe NC reduction occurs at ∼ −1.47 V (±0.01 V) in both experiments. Once CB electrons begin to accumulate, the change in E_F between $\langle n \rangle = 0$ and $\langle n \rangle = 1$ is small, with a slope of ∼ −10 mV/$\langle n \rangle$. The slope of E_F vs $\langle n \rangle$ increases as $\langle n_{max} \rangle$ is approached, and photodoping maximizes at $\langle n_{max} \rangle$ ∼ 1.4 and ∼ −1.52 V (±0.01 V) for both experiments. Plotted in this manner, the electrochemical data from these two experiments, which initially appeared markedly different (Figure 3B), are now essentially superimposable. From this result we conclude that the CdSe CB-edge potential is independent of the presence of Cp_2Co^+ under these conditions.

Comparing E_F data (Figures 2B and 3C), we note that the CdSe NCs at $\langle n \rangle = 1$ are ∼260 mV more reducing than the ZnO NCs at $\langle n \rangle = 1$ (−1.48 vs −1.22 eV, respectively). This difference is notably smaller than would be estimated from bulk data (∼1.1 eV, see SI), but it still indicates a driving force for inter-NC ET. To illustrate, a mixture of similar CdSe and ZnO NCs was prepared containing $Li[Et_3BH]$ as the hole quencher,[28] with all conditions similar to those of Figures 2 and 3. Figure 4 shows absorption spectra of this solution collected after selective CdSe photoexcitation for various durations. The broad NIR (<2 eV) absorption characteristic

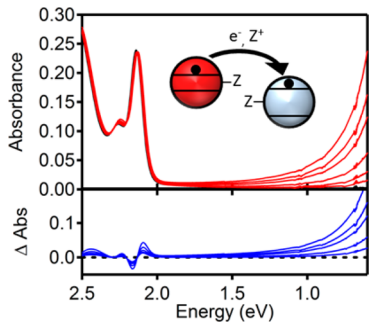

Figure 4. Top: Electronic absorption spectra of a mixture of d = 3.8 nm CdSe NCs (1.25 μM), d = 9.6 nm ZnO NCs (2 μM), and $Li[Et_3BH]$ (660 μM), collected after various durations of selective CdSe NC photoexcitation (broad-band, λ > 480 nm). Bottom: Difference spectra ($A - A_0$). For clarity, the data are plotted against energy (eV).

of n-ZnO (Figure 2A) grows with photoexcitation time. The CdSe excitonic absorption maximum redshifts by ∼20 meV over the same time window, but there is no evident bleach, allowing tentative attribution of this shift to a Stark effect associated with surface charge redistribution. Control experiments performed in the absence of CdSe NCs (see SI) show no spectroscopic changes, ruling out direct ZnO photodoping under these conditions. The absence of CdSe excitonic absorption bleach and growth of ZnO NIR absorbance indicate that photodoped CdSe NCs indeed transfer their electrons to ZnO NCs under these conditions, as anticipated from the favorable ET driving force measured electrochemically.

During the course of these experiments, several interesting complexities were noted. First, as anticipated from prior observations,[16,18] CdSe NC redox potentials are found to be extraordinarily sensitive to sample preparation and measurement conditions, varying reproducibly by hundreds of mV depending on the specific details. Consequently, the redox potentials reported here reflect the particular reaction conditions employed, just as standard reduction potentials ($E°$) of molecular reagents correspond to a standard set of conditions. These observations will be described in detail in a subsequent report, but this preliminary observation already highlights the utility of this technique for identifying sample-specific redox potentials through *in situ* measurements. Additionally, we found it possible to measure the potentials of sub-CB electron traps in CdSe NCs by combining potentiometry with photoluminescence spectroscopy (PL, see SI). Here, we observe PL brightening as E_F is raised, starting at least 120 mV below the CB edge, before the characteristic darkening that coincides with CB filling and the resulting Auger recombination.[20] NC PL brightening at sub-CB potentials is consistent with several recent observations[32−35] and indicates reductive passivation of surface electron traps. We note that in some cases CdSe NC surface-trap reduction appears to have exactly the opposite effect of quenching PL,[18,20,36] reflecting the complexity of these surface chemistries and highlighting the need for *in situ* electrochemical measurements.

Overall, the results presented here demonstrate potentiometry as a powerful and broadly applicable approach to semiconductor NC electrochemistry. With this approach, it is possible to quantify band-edge potentials *in situ*, without special apparatus or modification of NC surface chemistries. The impact of NC composition (isovalent or aliovalent impurities, etc.),[37−39] charge-compensating cations (H^+, Li^+, $[CoCp_2]^+$, etc.),[1,2,7,40] or NC surface ligands (with dipoles, conjugation, etc.)[16,18,41] should be readily quantified, and extension to other redox-active NC heterostructures[3,23] or nonphotochemical reductants appears equally promising. The transient potentiometry described by Figures 2 and 3 further suggests interesting possibilities for probing dynamical processes. NC potentiometry thus opens new opportunities for future fundamental and applied research involving redox-active colloidal semiconductor NCs.

■ ASSOCIATED CONTENT

Supporting Information

The Supporting Information is available free of charge on the ACS Publications website at DOI: 10.1021/jacs.6b00936.

Experimental details and data (PDF)

DOI: 10.1021/jacs.6b00936
J. Am. Chem. Soc. 2016, 138, 4310−4313

AUTHOR INFORMATION

Corresponding Author

*gamelin@chem.washington.edu

Notes

The authors declare no competing financial interest.

ACKNOWLEDGMENTS

This research was supported by the NSF (CHE-1506014 to DRG, Graduate Research Fellowship DGE-1256082 to KHH), NIH (Postdoctoral Fellowship F32GM110876 to EYT), and the State of Washington through the Clean Energy Institute via funding from the Washington Research Foundation (to CKB).

REFERENCES

(1) Dung, D.; Ramsden, J.; Grätzel, M. *J. Am. Chem. Soc.* **1982**, *104*, 2977.
(2) Nenadović, M. T.; Rajh, T.; Mićić, O. I.; Nozik, A. J. *J. Phys. Chem.* **1984**, *88*, 5827.
(3) Jakob, M.; Levanon, H.; Kamat, P. V. *Nano Lett.* **2003**, *3*, 353.
(4) Huang, J.; Stockwell, D.; Huang, Z.; Mohler, D. L.; Lian, T. *J. Am. Chem. Soc.* **2008**, *130*, 5632.
(5) Han, Z.; Qiu, F.; Eisenberg, R.; Holland, P. L.; Krauss, T. D. *Science* **2012**, *338*, 1321.
(6) Jensen, S. C.; Homan, S. B.; Weiss, E. A. *J. Am. Chem. Soc.* **2016**, *138*, 1591.
(7) Schimpf, A. M.; Knowles, K. E.; Carroll, G. M.; Gamelin, D. R. *Acc. Chem. Res.* **2015**, *48*, 1929.
(8) Ning, Z.; Voznyy, O.; Pan, J.; Hoogland, S.; Adinolfi, V.; Xu, J.; Li, M.; Kirmani, A. R.; Sun, J.-P.; Minor, J.; Kemp, K. W.; Dong, H.; Rollny, L.; Labelle, A.; Carey, G.; Sutherland, B.; Hill, I.; Amassian, A.; Liu, H.; Tang, J.; Bakr, O. M.; Sargent, E. H. *Nat. Mater.* **2014**, *13*, 822.
(9) Chuang, C.-H. M.; Brown, P. R.; Bulović, V.; Bawendi, M. G. *Nat. Mater.* **2014**, *13*, 796.
(10) Haram, S. K.; Quinn, B. M.; Bard, A. J. *J. Am. Chem. Soc.* **2001**, *123*, 8860.
(11) Inamdar, S. N.; Ingole, P. P.; Haram, S. K. *ChemPhysChem* **2008**, *9*, 2574.
(12) Amelia, M.; Lincheneau, C.; Silvi, S.; Credi, A. *Chem. Soc. Rev.* **2012**, *41*, 5728.
(13) Kucur, E.; Riegler, J.; Urban, G. A.; Nann, T. *J. Chem. Phys.* **2003**, *119*, 2333.
(14) Querner, C.; Reiss, P.; Sadki, S.; Zagorska, M.; Pron, A. *Phys. Chem. Chem. Phys.* **2005**, *7*, 3204.
(15) Vanmaekelbergh, D.; Liljeroth, P. *Chem. Soc. Rev.* **2005**, *34*, 299.
(16) Brown, P. R.; Kim, D.; Lunt, R. R.; Zhao, N.; Bawendi, M. G.; Grossman, J. C.; Bulović, V. *ACS Nano* **2014**, *8*, 5863.
(17) Jeong, K. S.; Deng, Z.; Keuleyan, S.; Liu, H.; Guyot-Sionnest, P. *J. Phys. Chem. Lett.* **2014**, *5*, 1139.
(18) Wang, C.; Shim, M.; Guyot-Sionnest, P. *Science* **2001**, *291*, 2390.
(19) Scanlon, M. D.; Peljo, P.; Mendez, M. A.; Smirnov, E.; Girault, H. H. *Chem. Sci.* **2015**, *6*, 2705.
(20) Rinehart, J. D.; Schimpf, A. M.; Weaver, A. L.; Cohn, A. W.; Gamelin, D. R. *J. Am. Chem. Soc.* **2013**, *135*, 18782.
(21) Schimpf, A. M.; Gunthardt, C. E.; Rinehart, J. D.; Mayer, J. M.; Gamelin, D. R. *J. Am. Chem. Soc.* **2013**, *135*, 16569.
(22) Haase, M.; Weller, H.; Henglein, A. *J. Phys. Chem.* **1988**, *92*, 482.
(23) Wood, A.; Giersig, M.; Mulvaney, P. *J. Phys. Chem. B* **2001**, *105*, 8810.
(24) Shim, M.; Guyot-Sionnest, P. *Nature* **2000**, *407*, 981.
(25) Shim, M.; Guyot-Sionnest, P. *J. Am. Chem. Soc.* **2001**, *123*, 11651.
(26) Liu, W. K.; Whitaker, K. M.; Smith, A. L.; Kittilstved, K. R.; Robinson, B. H.; Gamelin, D. R. *Phys. Rev. Lett.* **2007**, *98*, 186804.
(27) Carroll, G. M.; Schimpf, A. M.; Tsui, E. Y.; Gamelin, D. R. *J. Am. Chem. Soc.* **2015**, *137*, 11163.
(28) Prior work has established that photodoping using $[Et_3BH]^-$ is largely independent of alkali metal countercation (ref 21).
(29) Shim, M.; Wang, C.; Guyot-Sionnest, P. *J. Phys. Chem. B* **2001**, *105*, 2369.
(30) To account for the possibility of residual baseline effects, the spectra in Figure 3A were also analyzed by Gaussian fitting (see SI), from which $\langle n_{max} \rangle = 1.3$ is estimated.
(31) Partial reduction of Cp_2Co^+ by $Na[Et_3BH]$ was confirmed by optical detection of Cp_2Co even in the absence of CdSe NCs (not shown). Only a small portion of Cp_2Co^+ is reduced. This reduction likely involves an unidentified minority species in solution, because if direct reduction of Cp_2Co^+ by $Na[Et_3BH]$ were possible, then it would be expected to be irreversible and proceed to completion. In the presence of CdSe NCs, some Cp_2Co^+ reduction may also occur from inadvertent CdSe photoexcitation under normal handling conditions.
(32) Jha, P. P.; Guyot-Sionnest, P. *J. Phys. Chem. C* **2010**, *114*, 21138.
(33) Galland, C.; Ghosh, Y.; Steinbruck, A.; Sykora, M.; Hollingsworth, J. A.; Klimov, V. I.; Htoon, H. *Nature* **2011**, *479*, 203.
(34) Weaver, A. L.; Gamelin, D. R. *J. Am. Chem. Soc.* **2012**, *134*, 6819.
(35) Rinehart, J. D.; Weaver, A. L.; Gamelin, D. R. *J. Am. Chem. Soc.* **2012**, *134*, 16175.
(36) Gooding, A. K.; Gomez, D. E.; Mulvaney, P. *ACS Nano* **2008**, *2*, 669.
(37) Cohn, A. W.; Kittilstved, K. R.; Gamelin, D. R. *J. Am. Chem. Soc.* **2012**, *134*, 7937.
(38) Zhou, D.; Kittilstved, K. R. *J. Mater. Chem. C* **2015**, *3*, 4352.
(39) Schimpf, A. M.; Lounis, S. D.; Runnerstrom, E. L.; Milliron, D. J.; Gamelin, D. R. *J. Am. Chem. Soc.* **2015**, *137*, 518.
(40) Valdez, C. N.; Braten, M.; Soria, A.; Gamelin, D. R.; Mayer, J. M. *J. Am. Chem. Soc.* **2013**, *135*, 8492.
(41) Frederick, M. T.; Weiss, E. A. *ACS Nano* **2010**, *4*, 3195.

DOI: 10.1021/jacs.6b00936
J. Am. Chem. Soc. 2016, 138, 4310−4313